Shading Correction for Whole Slide Image Using Low Rank and Sparse Decomposition

Tingying Peng[1,3], Lichao Wang[1,4], Christine Bayer[5], Sailesh Conjeti[1,6], Maximilian Baust[1], and Nassir Navab[1,2]

[1] Computer Aided Medical Procedures (CAMP), Technische Universität München, Germany
[2] Computer Aided Medical Procedures (CAMP), Johns Hopkins University, USA
[3] Department of Nuclear Medicine, Technische Universität München, Germany
[4] Helmholtz Zentrum München, Germany
[5] Department of Radiation Oncology, Technische Universität München, Germany
[6] School of Medical Science and Technology, IIT Kharagpur, India

Abstract. Many microscopic imaging modalities suffer from the problem of intensity inhomogeneity due to uneven illumination or camera nonlinearity, known as shading artifacts. A typical example of this is the unwanted seam when stitching images to obtain a whole slide image (WSI). Elimination of shading plays an essential role for subsequent image processing such as segmentation, registration, or tracking. In this paper, we propose two new retrospective shading correction algorithms for WSI targeted to two common forms of WSI: multiple image tiles before mosaicking and an already-stitched image. Both methods leverage on recent achievements in matrix rank minimization and sparse signal recovery. We show how the classic shading problem in microscopy can be reformulated as a decomposition problem of low-rank and sparse components, which seeks an optimal separation of the foreground objects of interest and the background illumination field. Additionally, a sparse constraint is introduced in the Fourier domain to ensure the smoothness of the recovered background. Extensive qualitative and quantitative validation on both synthetic and real microscopy images demonstrates superior performance of the proposed methods in shading removal in comparison with a well-established method in ImageJ.

1 Introduction

Automated microscopic image processing and analysis are increasingly gaining attention in the field of biological imaging. However, a common artifact that encumbers the use of automatic image processing techniques is intensity inhomogeneity present in microscopic images, also known as shading [1]. Intensity inhomogeneity may originate from non-uniform illumination, uneven sample thickness or camera nonlinearity. As shown in Fig. 1(a), the shading effect manifests itself in whole slide image (WSI) by introducing unwanted seams in stitched mosaics.

In general, shading can be categorized into object-dependent and object-independent shading [2]. A careful prospective calibration process may solve object-independent shading, e.g. by using a calibration slide, which is, however, not always available. More commonly, posteriori (retrospective) image processing algorithms are developed to correct both object-dependent and object-independent shading.

P. Golland et al. (Eds.): MICCAI 2014, Part I, LNCS 8673, pp. 33–40, 2014.

Existing popular retrospective shading correction methods include morphological filtering [3], Gaussian blurring [4], entropy minimization [5] or fitting polynomial surfaces [6]. Some of these methods are not fully automatic, e.g. the control points for the polynomial fitting should not be positioned on the objects, which require either manual interference or object-dependent segmentation. Moreover, it has been shown that the performance of the majority of these methods is strongly affected by the size of the foreground objects [2]. Due to the increased magnification in WSI, the foreground objects in each image tile are enlarged and can therefore negatively affect the performance of conventional shading correction algorithms.

Apart from above mentioned algorithmic limits, there is an additional constraint for shading correction of WSI in practice. The output of currently popular whole slide microscopy scanning devices comes usually in two forms, namely a sequence of tile images that need to be stitched into the WSI or an already-stitched WSI. Shadings exist in both forms. Therefore, we propose two automatic algorithms to remove shading effects of WSI, one for each form of the output image. Both these algorithms are based on approximating the foreground objects and the background illumination field by a sparse and a low rank matrix, respectively. Both algorithms were evaluated qualitatively and quantitatively using synthetic and real microscopic images.

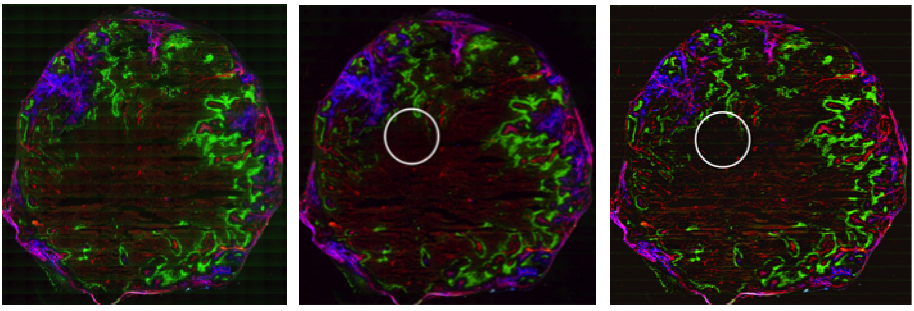

Fig. 1. (Left) the mosaic built using the original (uncorrected) fluorescence image sequences, which reveals strong illumination discontinuity across the stitching borders in the green channel; (middle) shading correction using Algorithm 1 successfully removes this artifact and achieves a seamless mosaicking; (right) artifact remains after "Rolling Ball" correction.

2 Methods

2.1 Modelling the Shading Effect in Microscopy

The effect of shading on microscope image intensities is typically based on either a multiplicative model or an additive model of the artifact [2]:

$$I(x,y) = O(x,y) \cdot S(x,y) \tag{1}$$

$$I(x,y) = O(x,y) + S(x,y) \tag{2}$$

where I and O are the observed and the true stain-related image intensities respectively and S is the distortion caused by shading. By taking the logarithm of the image

intensities: $\hat{I}(x,y) = log\big(I(x,y)\big)$, Equation 1 becomes $\hat{I} = \hat{O} + \hat{S}$, thus being the additive model. By taking the exponent of the additive model we can also jump back to the multiplicative one. Hence, although the following proposed illumination correction methods are based on the additive model, it is straightforward to be transferred into a multiplicative one. In the additive model, the shading-free image O is also denoted as the foreground, F, whilst the shading field is denoted as the background, B.

2.2 Shading Correction of WSI Using Multiple Image Tiles

In this subsection the first proposed algorithm (Algorithm 1) is described. In case of the whole slide image, a series of images, $I_1, I_2, \ldots, I_n$, are collected using the same microscope with the same settings. Hence they share the same background illumination field, $I_i = F_i + B$. Generally, the foreground F_i occupies only a fraction of the image pixels and therefore can be treated as a *sparse* component. If we concatenate each image into a column vector, the observation model can be written as:

$$D \stackrel{\text{def}}{=} [\text{vec}(I_1)|\cdots|\text{vec}(I_n)] = A + E \tag{3}$$

where $A = [\text{vec}(B)|\cdots|\text{vec}(B)] \in \mathbb{R}^{m\times n}$ is a *low rank (rank one)* matrix that models the common background of each image. And $E = [\text{vec}(F_1)|\cdots|\text{vec}(F_n)] \in \mathbb{R}^{m\times n}$ is the sparse signal matrix. Hence, we can solve the following minimization problem:

$$\min_E \|E\|_1, \text{s.t.}\, D = A + E, a_i = a_j \tag{4}$$

where $\|\cdot\|_1$ denotes the l_1-norm (i.e. the sum of the absolute values of matrix elements). a_i is the ith column of matrix A, and $a_i = a_j$ forces the estimated background field from each image to be the same. Moreover, it is also reasonable to assume the background illumination field to be smooth. Smooth functions are typically sparse in the Fourier transformed domain. We could modify the above convex optimization problem (3) as follows to impose this additional smoothness constraint:

$$\min_{W,E} \|W\|_1 + \|E\|_1, \quad \text{s.t.}\, D = A + E, A = \text{repmat}(QWQ^T) \tag{5}$$

where $\text{repmat}(QWQ^T) \stackrel{\text{def}}{=} [\text{vec}(QWQ^T)|\cdots|\text{vec}(QWQ^T)]$ (repeated n times) and Q is chosen to be discrete cosine transform (DCT). W is the matrix of the DCT coefficients and fulfills the sparse constraint.

Solving (4) requires simultaneously minimization of l_1-norm of two matrices, in the original and Fourier spaces respectively. Here we utilize the Linearized Alternating Direction Method (LADM), which is widely used in solving various low-rank and sparse matrix separation and recovery problems (e.g. robust PCA in [7])

$$\begin{aligned} L(W,E,Y,\mu) = \|W\|_1 + \|E\|_1 + \langle Y, D - \text{repmat}(QWQ^T) - E\rangle \\ + \mu\|D - \text{repmat}(QWQ^T) - E\|_F \end{aligned} \tag{6}$$

Here Y denotes the Lagrange multiplier, $\langle\cdot,\cdot\rangle$ is the inner product, $\|\cdot\|_F$ is the Frobenius norm and $\mu > 0$ is a penalty parameter. Incorporating the LADM updating scheme, the proposed Algorithm 1 is described as the following:

Algorithm 1 (Shading correction of WSI using multiple image tiles)

Input: Observation matrix $D \in \mathbb{R}^{m \times n}$, each column of matrix D corresponds to a concatenated vector of each image.

1: $Y_0 = D/J(D)$; $W_0 = 0$; $E_0 = 0$; $\mu_0 > 0$; $\rho > 1$; $k = 0$.

2: **while** not converged **do**

3: $W_{k+1} = \boldsymbol{T}_{\mu_k^{-1}}\{W_k + Q^T[\text{avg}(D - \text{repmat}(QW_kQ^T) - E_k + Y_k/\mu_k)]Q\}$;

4: $E_{k+1} = \boldsymbol{T}_{\mu_k^{-1}}\{D - \text{repmat}(QW_{k+1}Q^T) + Y_k/\mu_k\}$;

5: $Y_{k+1} = Y_k + \mu_k(D - \text{repmat}(QW_{k+1}Q^T) - E_{k+1})$; $\mu_{k+1} = \rho\mu_k$, $k = k + 1$.

6: **end while**

7: **Output:** (W_k, E_k); QW_kQ^T is the estimated background illumination field.

Where $\text{avg}(\cdot)$ is the mean column of the matrix and $\boldsymbol{T}_\varepsilon(x) = \text{sgn}(x)\max(|x| - \varepsilon, 0)$ is the scalar shrinkage operator, $J(x)$ is the dual norm of x (for details refer to [8]).

2.3 Shading Correction of an Already Stitched WSI

In this subsection the proposed Algorithm 2 is described. Instead of providing tile image sequence, many WSI microscopy scanners output only an already-stitched WSI. In such a case, it is generally difficult to recover tile images without the prior knowledge of the detailed microscopy acquisition and stitching protocol and hence Algorithm 1 can no longer be used. We notice in previous studies that the smoothly varying background illumination field is often modeled using limited terms of some basis function, e.g., second-order polynomials [5]

$$B(x, y) = a_0 + a_1x + a_2y + a_3xy + a_4x^2 + a_5y^2 \tag{7}$$

It can be seen that the estimated illumination field using polynomials has a low rank ($rank(B) \leq 5$). For a WSI that is stitched from a microscopy sequence, its illumination field is simply a repeating pattern of individual background and hence is also low rank. However, as suggested in [9], being low-rank *does not necessarily imply smoothness*. Therefore, similar to Algorithm 1, we introduce a smoothness constraint, which can be interpreted as the estimated background to be *low rank as well as sparse in the Fourier domain*. In this circumstance, the optimization problem becomes ([9]):

$$\min_{A,E,W} \|A\|_* + \gamma\|W\|_1 + \lambda\|E\|_1, \text{s.t.}\, D = A + E, A = QWQ^T \tag{8}$$

where $\|\cdot\|_*$ represents the nuclear norm of a matrix (i.e. the sum of the matrix singular values), γ controls the smoothness of the estimated background whilst λ controls the relative sparsity of the foreground. The optimal settings for γ and λ depend on the characteristics of the processed image and will be explained in the results section. Again, we use LADM to solve the optimization problem (Algorithm 2).

3 Experiments and Results

In this section we evaluate the qualitative and quantitative performance of the proposed correction methods on both synthetic and real microscopic images. Further,

Algorithm 2 (Shading correction for an already-stitched WSI)

Input: Observation image $D \in \mathbb{R}^{m\times n}$.
1: $Y_{10} = 0; Y_{20} = D/J(D);\ A_0 = 0;\ W_0 = 0; E_0 = 0; \mu_0 > 0; \rho > 1; k = 0.$
2: **while** not converged **do**
3: $W_{k+1} = \boldsymbol{T}_{\gamma/\mu_k}\{W_k + Q^T[D + A_k - E_k - 2QW_kQ^T + Y_{1k}/\mu_k + Y_{2k}/\mu_k]Q\};$
4: $E_{k+1} = \boldsymbol{T}_{\lambda/\mu_k}\{D - QW_{k+1}Q^T + Y_{2k}/\mu_k\};$
5: $(U,S,V) = \text{svd}(QW_{k+1}Q^T - Y_{1k}/\mu_k);\ A_{k+1} = U\boldsymbol{T}_{\mu_k^{-1}}(S)V^T;$
6: $Y_{1k+1} = Y_{1k} + \mu_k(A_{k+1} - QW_{k+1}Q^T);\ Y_{2k+1} = Y_{2k} + \mu_k(D - QW_{k+1}Q^T - E_{k+1});$
7: $\mu_{k+1} = \rho\mu_k;\ k = k + 1.$
8: **end while**
9: **Output:** (A_k, E_k); A_k is the estimated illumination field and E_k is the corrected image with uniform illumination.

we compare our two methods with the "Rolling Ball" shading correction algorithm in ImageJ [10], which achieves the best performance amongst several popular retrospective shading correction methods [11]. For WSI image tiles, "Rolling Ball" is used to estimate a shading field of each image tile separately and the common shading is taken as the median of individually estimated shading fields [12]; for an already-stitched WSI, "Rolling Ball" is used to correct the shading effect of a single image.

3.1 Test on Synthetic Data

Firstly, both the proposed shading correction strategies are tested by using true uniform microscopic images, simulating the shading effect, correcting the images, and comparing the corrected and the original images. For this purpose, 10 synthetic shading-free fluorescence microscopy images (1200x1200 pixels, normalized intensity between 0 and 1) are generated using the simulation tool presented in [13]. For each image, a background illumination field was simulated by the polynomial background model (Eq.8, $a_i \sim \mathcal{U}(0,1)$, maximum amplitude 0.2). The illumination field is used to corrupt the test image according to the additive shading model [13]. The WSI is imitated by dividing an image into multiple tiles using regular grids at a size of $n \times n$, with the same illumination field added to each image tile. Fig. 2 shows a synthetic WSI image without shading (left) and one with shading artifact (right). In the simulation study, we $\gamma = 0.1, \lambda = 0.05$ in Algorithm 2 and the rolling ball radius is set to be 100 pixels, which is about the size of the largest object of interest.

The quantitative performance of the proposed methods is measured by Mean Absolute Error (MAE), defined as the average of the absolute difference between the corrected image and the original shading-free image. Since both image simulation and shading correction are based on the additive model, the MAE of the foreground is equivalent to the error between the estimated and true backgrounds. As shown in Fig. 3, if the image is stitched from a very limited number of image tiles (e.g. 2x2), the Rolling Ball algorithm achieves good performance, which, however, deteriorates rapidly as the stitching size of the WSI increases. This is due to the fact that the Rolling Ball cannot separate the objects of interest if they are similar in size to the variations in the background. In contrast, the two proposed algorithms achieve consistently

good results, which demonstrates the effectiveness of the formulation of WSI shading as a low rank matrix in both cases. It is also illustrated that Algorithm 1 using multiple image tiles performs slightly better than Algorithm 2 using a stitched image.

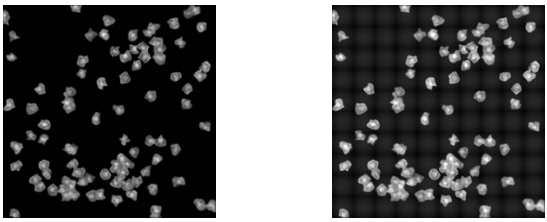

Fig. 2. The synthetic WSI with uniform (left) and uneven (right) illumination

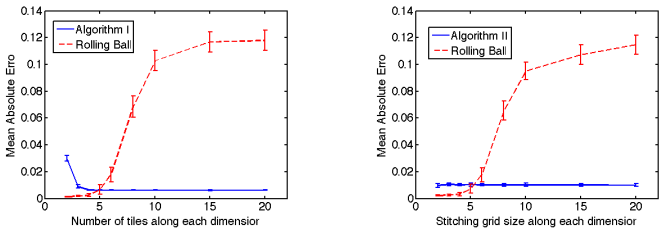

Fig. 3. Mean Absolute Error between the corrected and the reference microscopic image using Algorithm 1 on image tiles (left) and Algorithm 2 on an already-stitched WSI (right)

3.2 Shading Correction in WSI for Seamless Image Mosaic

The proposed algorithms are further evaluated in shading correction of 10 real WSIs (each WSI has a tile size of 50-200). These images were acquired using the MosaiX and Multidimentional acquisition modules of the Axiovision Program (Version 4.8.3.0; Zeiss). The false RGB colors encode AlexaFluor594, FITC-labeled anti-pimonidazole antibody and Hoechst33342 dyes respectively. The strong background shading is presented only in the green channel (Fig .1 left) because of the weak FITC fluorescence as well as its long exposure time. Algorithm 1 is used to perform shading correction, which removes the Moiré pattern artifact originally presented in the green channel completely without corrupting the shading-free red and blue channels (Fig. 1, middle). In contrast, the Rolling Ball algorithm (rolling radius 50 pixels) rejects a part of the red fluorescence (in white circle) as background (Fig.1. right). Besides visual inspection, the quality of our shading correction algorithm is further assessed using root-mean-square error (RMSE) on the overlap regions, a popular criteria to measure the mosaic quality of fluorescence microscopy [1]. As reported in Table 1, a Wilcoxon Signed Rank test indicates that our approach improves over the uncorrected images with high confidence. Although statistical significance is also achieved with the Rolling Ball algorithm, the average improvement (24.2%) is not as good as ours (35.8%).

The second example shown here is a stitched WSI of phase contrast image of neurons. Background non-uniformity is presented in each image tile and between tiles

(Fig. 4 (left)). Shading correction of this image is challenging due to the fact that the light diffraction in the background correlates with the foreground, making it difficult to remove the shading by prospective calibration. Secondly, the foreground consists of both bright and dark objects of difference sizes and hence the fundamental assumption of Rolling Ball algorithm is invalid here (Rolling Ball assumes the foreground is either brighter or darker than the background). By using sparse and low rank decomposition in Algorithm 2 ($\gamma = 0.1, \lambda = 0.005$), the foreground (middle) and background (right) are successfully separated for such a challenging case.

3.3 Discussion of the Results

Amongst the two proposed shading correction methods, Algorithm 1 is a blind method that does not require any user-setting parameters. In Algorithm 2, γ controls the smoothness of the estimated background and we determined that a fixed 0.1 works well for both our synthetic and real microscopy images. In comparison, λ needs to be tuned by users as it is related to the relative proportion of the foreground objects. In practice, this parameter can be fixed for a group of microscopy images collected from a particular experiment, as this proportion does not usually vary by much.

An ideal shading correction algorithm would correct artifact without distorting the underlying biological structures. The synthetic study has quantitatively demonstrated a minuscule error between the corrected image and the ground-truth biology. In the real image study, besides RMSE improvement in the shading-affected green channel, our algorithm does not corrupt the shading-free red and blue channels, which clearly shows that the relevant biological information is preserved. In fact, the low rank and sparse decomposition is completed so that no information is lost. In contrast to a low-rank background, biological structures are unlikely to have a low rank, being falsely removed by our algorithm.

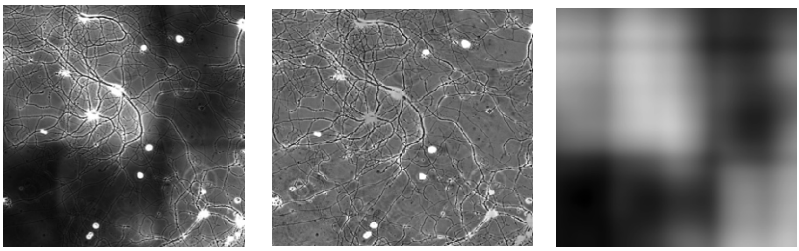

Fig. 4. Part of a WSI without (left) and with (middle) shading correction using Algorithm 2 and the estimated background illumination (right)

Table 1. RMSE on the overlap regions of WSI image tiles with and without shading removal

Mosaic set	Uncorrected	Algorithm 1	Rolling Ball
RMSE	12.0±2.5	7.7±1.4	9.1±1.7
p-value		0.002	0.03
Average Improvement		35.8%	24.2%

4 Conclusion

In this paper we propose two automatic algorithms to correct shading effect in whole slide microscopic imaging. These algorithms decompose a multi-image sequence (Algorithm 1) or an already-stitched image (Algorithm 2) into a background component approximated by a low rank matrix and a foreground component represented by a sparse matrix. In addition, the sparse constraint in the Fourier domain regularizes the smoothness of the recovered background. Both qualitative and quantitative evaluation using synthetic and different types of real microscopic images proves the accuracy of our methods as well as their generality.

Acknowledgement. T. Peng was supported by the Humboldt Research Fellowship (3.5-CHN/1149232 STP). The project was partially supported by SFB824. The authors would also like to thank Christophe Leterrier of Aix Marseille University, France to kindly provide the phase-contrast microscopic image.

References

1. Piccinini, F., Bevilacqua, A., Smith, K., Horvath, P.: Vignetting and photo-bleaching correction in automated fluorescence microscopy from an array of overlapping images. In: 2013 ISBI, pp. 464–467. IEEE (2013)
2. Tomazevic, D., Likar, B., Pernus, F.: Comparative evaluation of retrospective shading correction methods. J. Microsc. 208, 212–223 (2002)
3. Sternberg, S.R.: Biomedical Image Processing. IEEE Comput. 16, 22–34 (1983)
4. Leong, F.J.W.-M., Brady, M., McGee, J.O.: Correction of uneven illumination (vignetting) in digital microscopy images. J. Clin. Pathol. 56, 619–621 (2003)
5. Likar, B., Maintz, J.B., Viergever, M.A., Pernus, F.: Retrospective shading correction based on entropy minimization. J. Microsc. 197, 285–295 (2000)
6. Russ, J.C.: The Image Processing Handbook, 6th edn. CRC Press (2011)
7. Cand, E.J., Li, X., Ma, Y., Wright, J.: Robust Principal Component Analysis? (2009)
8. Lin, Z., Chen, M., Ma, Y.: The Augmented Lagrange Multiplier Method for Exact Recovery of Corrupted Low-Rank Matrices. In: NIPS (2011)
9. Liang, X., Ren, X., Zhang, Z., Ma, Y.: Repairing sparse low-rank texture. In: Fitzgibbon, A., Lazebnik, S., Perona, P., Sato, Y., Schmid, C. (eds.) ECCV 2012, Part V. LNCS, vol. 7576, pp. 482–495. Springer, Heidelberg (2012)
10. Collins, T.J.: ImageJ for microscopy. Biotechniques 43, 25–30 (2007)
11. Babaloukas, G., Tentolouris, N., Liatis, S., Sklavounou, A., Perrea, D.: Evaluation of three methods for retrospective correction of vignetting on medical microscopy images utilizing two open source software tools. J. Microsc. 244, 320–324 (2011)
12. Piccinini, F., Lucarelli, E., Gherardi, A., Bevilacqua, A.: Multi-image based method to correct vignetting effect in light microscopy images. J. Microsc. 248, 6–22 (2012)
13. Lehmussola, A., Ruusuvuori, P., Selinummi, J., Huttunen, H., Yli-Harja, O.: Computational framework for simulating fluorescence microscope images with cell populations. IEEE Trans. Med. Imaging 26, 1010–1016 (2007)